JST: Engineering and Technology for Sustainable Development
Volume 34, Issue 1, March 2024, 019-026

Investigation of Thermal Decomposition and Thermal Oxidative Degradation of a Composite of Cellulose Nanofibers and Deproteinized Natural Rubber Grafted Methyl Methacrylate

Nguyen Thi Quynh, Nguyen Thi Ngoc, Le Quang Dien, Nguyen Thu Ha, Tran Thi Thuy, Nguyen Ngoc Mai*
Hanoi University of Science and Technology, Ha Noi, Vietnam
**Corresponding author email: mai.nguyenngoc@hust.edu.vn*

Abstract

Natural rubber (NR) is a polymer that has many applications in daily life. However, the traditional rubber industry relies heavily on petroleum-based materials, causing environmental pollution problems. Therefore, to reduce environmental challenges, products created from NR are combined with non-toxic chemicals and natural fillers such as cellulose nanofibers (CNF). This study presents the effect of CNF on the thermal properties of novel composites made from CNF and deproteinized natural rubber grafted methyl methacrylate (DPNR-g-MMA) under air and nitrogen atmosphere. Graft copolymerization of MMA onto DPNR to produce DPNR-g-PMMA was performed in the latex phase. The CNF/DPNR-g-PMMA composite was created by dispersing CNF in DPNR-g-PMMA at ratios of 0.5%, 1%, and 1.5% using ultrasonic waves. DPNR-g-PMMA was employed as the composite's matrix and CNF served as its reinforcing phase. Fourier transform infrared spectroscopy (FTIR) and proton nuclear magnetic resonance spectroscopy (^{1}H NMR) were used to confirm the success of the graft copolymerization. The thermal properties of materials were studied by Thermalgravimetric analysis (TGA) and Differential scanning calorimetry (DSC), in which the thermal stability of composites was examined via TGA under air and nitrogen atmosphere. The obtained data illustrate that, in comparison to DPNR and DPNR-g-PMMA, the decomposition temperature of all CNF/DPNR-g-PMMA composites, especially at CNF ratio of 1%. After blending CNF to DPNR-g-PMMA, the decomposition temperatures of CNF/DPNR-g-PMMA 1% increased by nearly 2 °C in nitrogen atmosphere and by 5.27 °C in air atmosphere. These results prove that the CNF is a key role in the thermal stability of DPNR-g-PMMA.

Keywords: Cellulose nanofibers, deproteinized natural rubber, methyl methacrylate, thermal degradation, thermal oxidative degradation.

1. Introduction

Natural rubber (NR) from Hevea Brasiliense trees composed of 93-95% cis-1,4-polyisoprene [1, 2]. It is an important material in the rubber industry with possesses superior properties such as high strength, outstanding resilience, and high elongation at break [1, 3]. This biopolymer has a wide range of applications in areas such as conveyor belts, engine mounts, hoses, gaskets, rubber thread, tires, foam, and adhesives...[4]. However, the carbon-carbon double bonds in the NR backbone make them vulnerable to deterioration when exposed to sunshine, ozone, UV radiation, and air, particularly at high temperatures [2]. Therefore, NR is typically combined with a variety of additives, including fillers, vulcanizing agents, antioxidants, etc. to improve the desired properties [4]. The use of fillers has attracted considerable attention of researchers because the reinforcement effect is achieved through partial immobilization of polymer chains, thus improving the resistance against chain slippage which in turn enhances the mechanical performance of NR [4]. Carbon black (CB), silica, kaolin, and synthetic fibers are a few examples of fillers [4]. Because of their minuscule size, these materials have a restricted ability to disperse. Furthermore, CB poses a health concern to humans due to its carcinogenic potential. Therefore, it is necessary to look for fillers to replace them.

In recent times, there has been significant attention towards natural fiber-based fillers, appreciated for their environmentally friendly nature, sustainable sourcing of feedstock, and capacity to reinforce polymer matrices. One of the outstanding components of natural fibers that stands out is cellulose. It is made up of 1,4-linked glucose molecules and is a linear homopolymer [5]. It is known that is a fascinating and almost inexhaustible and sustainable natural polymeric raw material characterized by exciting properties such as including high mechanical properties, biodegradability, high strength, high aspect ratio, high specific surface area, low thermal expansion, and low density [5]. Therefore,

ISSN 2734-9381
https://doi.org/10.51316/jst.172.etsd.2024.34.1.3
Received: 21 Nov 2023; revised: 26 Dec 2023;
accepted: 26 Dec 2023

cellulose nanomaterial such as cellulose nanofibers (CNF) offers significant promise when used as reinforcement for NR.

The combination of CNF and NR is expected to improve the disadvantages of NR. Nevertheless, the hydrophilic nature of cellulose could be the major drawback of their application in hydrophobic polymer matrices [5]. This can be explained by the fact that there is little intermolecular mixing between the phases of two polymers [6]. Consequently, the cellulose fibers exhibit poor dispersion within the natural rubber matrix, facilitating agglomeration and resulting in a composite with inferior mechanical properties. In addressing this challenge, immiscible blends are frequently compatibilized [7]. The primary objective of compatibilization techniques is to stabilize the morphology and enhance adhesion between the phases in immiscible blends. To achieve this, compatibilizers, often in the form of block or graft copolymers, have been demonstrated as effective means [8]. Commonly, compatibilization enhances interfacial adhesion in which it may form an interface between the phases. Consequently, this enhancement in interfacial adhesion contributes to the overall improvement in mechanical properties. Nowadays, enhancing compatibility involves polarizing NR through the vinyl-monomer grafting technique. Acrylonitrile (AN) [9], methyl methacrylate (MMA) [3], maleic anhydride (MA) [10] are among the prominently used vinyl monomers. Of these, MMA stands out as the most suitable option for grafting with NR due to its superior grafting efficiency, resulting in significantly improved thermal mechanical properties of NR.

The use of MMA for graft polymerization to chemically modify NR, followed by reinforcement with CNF, holds enormous potential for enhancing the thermal characteristics of NR. Up to now, there has been no report on the combination of CNF and deproteinized natural rubber grafted methyl methacrylate (DPNR-g-PMMA) as well as studying the properties of CNF/DPNR-g-PMMA materials. Most especially, the thermal properties of the material have a great influence on the application in the material manufacturing industries. It was previously reported to show significant thermal improvement of natural rubber after protein removal and graft copolymerization with vinyl monomers [2, 3]. Thus, the thermal properties of DPNR-g-PMMA after being reinforced with CNF should be investigated carefully. Since NR is easily degraded by heat and oxidation when exposed to oxygen, the thermal properties of CNF/DPNR-g-PMMA composites need to be investigated in different environments. Therefore, the thermal degradation behavior of the material was investigated using thermogravimetric analysis in both nitrogen and air atmosphere.

In this research, the graft copolymerization of MMA onto deproteinized natural rubber (DPNR) was successfully performed. The structure of DPNR-g-PMMA was confirmed by proton nuclear magnetic resonance spectroscopy (^{1}H NMR) and attenuated total reflection-Fourier transform infrared spectroscopy (ATR-FTIR). CNF/DPNR-g-PMMA materials with different ratios were obtained by dispersing CNF into DPNR-g-PMMA with the help of ultrasonic waves. The thermal properties of those samples were studied via differential scanning calorimetry (DSC) and thermogravimetric analysis (TGA). The thermal stability of the material was analyzed in nitrogen and air atmosphere.

2. Experiment

2.1. Materials

High ammonium natural rubber (HANR) latex containing 60% dried rubber content (DRC) was provided by Merufa Company (Ho Chi Minh city, Vietnam). Cellulose nanofibers (CNF) were obtained from *Oryza sativa L.* rice straw using combined treatment by hydrogen peroxide and dilute sulfuric acid solution according to [11] was supplied from Dept. of Cellulose and Paper Tech. (HUST, Vietnam). Sodium dodecyl sulfate (SDS) (>97.0%) was purchased from Tokyo Chemical Industry Co., Ltd. (Tokyo, Japan). Urea (≥99.0%) was obtained from Nacalai Tesque, Inc (Kyoto, Japan). Methyl methacrylate (MMA), tert-(butyl hydroperoxide (TBHPO) (70 *wt.*% in H_2O), and tetra-ethylenepentamine (TEPA) were supplied by Sigma-Aldrich Chemie Gmbh (Munich, Germany). Sodium hydroxide was purchased Merck. Acetone, Ethanol, and Methyl Ethyl Ketone (MEK) were supplied by Xilong (China).

2.2. Methods

2.2.1. Preparation of DPNR latex and graft copolymer

DPNR was prepared from a fresh high ammonium natural rubber (HANR) latex containing 60% dried rubber content (DRC) by incubating the latex with 0.1 *wt.*% urea and 1 *wt.*% SDS at room temperature for 1 hour, followed by centrifugation at 10,000 rpm for 30 min at 15 °C. After centrifugation, the cream fraction was separated and dispersed in 1 *wt.*% SDS solution to make 30% DRC latex. The latex was washed two more times by centrifugation before obtaining the final DPNR, which was dispersed and preserved, respectively, in a 1 *wt.*% SDS. This level of SDS concentration in DPNR latex was used for graft copolymerization with MMA to avoid coagulation of colloidal suspensions.

DPNR latex (DRC 30%) was introduced into a 500 mL glass reaction vessel equipped with a mechanical stirrer, then flushed with argon gas for one hour, stirring at 250 rpm at 30 °C to remove dissolved oxygen in latex. The experiment was continued by adding a ratio 1:1 redox initiator system at a

concentration of 6.6 × 10^{-5} mol/g rubber. After that, pure MMA monomer was slowly added (at a concentration of 15 *wt.*% MMA per kg of rubber) to the reaction system [3]. Then the reaction was carried out for 2.5 h at 30 °C with continuously stirring at 400 rpm. Immediately after completion of the graft copolymerization, the unreacted monomer was removed in a rotary evaporator under reduced pressure. The finished latex was diluted to 30% DRC and mixed with 0.5%, 1%, and 1.5% ratios of CNF in the following step. The mixtures were then dried to a constant mass under reduced pressure at 50 °C for 2 weeks which contained homopolymers was obtained. DPNR-g-PMMA and CNF/DPNR-g-PMMA were further purified by Soxhlet extraction using MEK/acetone (3:1) solvent system to remove PMMA homopolymer.

2.2.2. Preparation of CNF/DPNR-g-PMMA composite

CNF with ratios of 0.5%, 1%, and 1.5% was dispersed in DPNR-g-PMMA latex by applying ultrasonic waves with 50% amplitude [12, 13] at 25 °C for 10 minutes. After that, the CNF/DPNR-g-PMMA mixture was poured into glass plates and oven dried at 50 °C for 2 weeks to obtain a dry film of 1 mm thickness. The resulting films were conditioned at room temperature in desiccators containing P_2O_5 until testing. The schematic to perform the CNF/DPNR-g-PMMA synthesis is shown in Fig. 1.

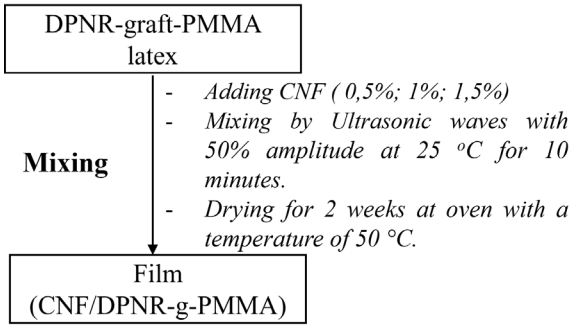

Fig. 1. Synthesis process of CNF/DPNR-g-PMMA composite

2.3. Characterization Methods

Fourier transform infrared spectroscopy (FTIR) was used for the analysis of the DPNR, DPNR-g-PMMA and CNF/DPNR-g-PMMA 1% samples with a scan range of 400 cm^{-1} to 4000 cm^{-1}. The samples were recorded on a Nicolet iS50 with attenuated total reflection mode.

Proton nuclear magnetic resonance (^{1}H NMR) spectra were recorded on a JEOL JNM-ECA 400 MHz spectrometer. For this measurement, dried rubber was firstly swelled in Chloroform-D for 1 week before being subjected to the spectrometer.

The glass transition temperatures of DPNR, DPNR-g-PMMA and CNF/DPNR-g-PMMA were studied by differential scanning calorimetry (DSC) using a DSC 7020 Exostar analyzer. The samples were cooled down to -150 °C using liquid nitrogen and heated up to 120 °C at a constant rate of 10 °C/min. The glass transition temperature, determined by ASTM E 2602 [14] standard, was identified using a tangent constructed to the baseline before and after the glass transition. Tangents were drawn at the inflection point during the glass transition, corresponding to the maximum slope. These tangents were extended until intersecting with the baselines, denoted as T_1 and T_2. The glass transition temperature (T_g) was computed as $T_g = (T_1 + T_2)/2$.

Thermal gravimetric analysis (TGA) experiments were performed using a NETZSCH STA 449F5 analyzer with a heating rate of 10 °C/min under nitrogen and air atmospheres and a temperature scan of 25 °C - 600 °C.

3. Results and Discussion

3.1. Characterization of CNF/DPNR-g-PMMA

The successful grafting of MMA onto DPNR was confirmed by ^{1}H NMR using Chloroform-D ($CDCl_3$) as a solvent of the measurement (Fig. 2).

For the structure of poly(cis-isoprene), unsaturated methine (-CH=) proton shows a singlet resonance signal at 5.11 ppm. The peak at 2.03 ppm may be attributed to the methylene (-CH_2-) protons and the resonance signal of the methyl (-CH_3) proton appears at 1.68 ppm [1, 2, 15]. The peak for standard solvent (deuterated chloroform) was observed at 7.26 ppm. Apart from those characteristic signals of cis-1,4-isoprene, an additional signal at about 3.60 ppm was assigned to the proton of methoxy (-OCH_3-) of the acrylic in the DPNR-g-PMMA copolymer [3].

The structure of the DPNR-g-PMMA copolymer was further demonstrated by comparing its FTIR signal with that of DPNR in Fig. 3.

The absorption bands of DPNR and DPNR-g-PMMA correspond to the structure of polyisoprene which was characterized by signals: C_{sp3}-H stretching vibration at 2956 cm^{-1}, C=C bending vibration at 841 cm^{-1}, C=C stretching vibration at 1450 cm^{-1} and C-H bending vibration at 1375 cm^{-1}. In addition to typical absorption frequencies for NR, the FTIR spectra of DPNR-g-PMMA revealed new signals associated with corresponding grafted copolymers.The additional peak at 1730 cm^{-1} was assigned to the valence vibration of the C=O (carbonyl groups) when MMA was grafted on the natural rubber backbone [3]. This is strong evidence to confirm the presence of the PMMA segment in DPNR-g-PMMA. Therefore, the combination of ^{1}H NMR data and FTIR results can be concluded that graft copolymerization was performed successfully.

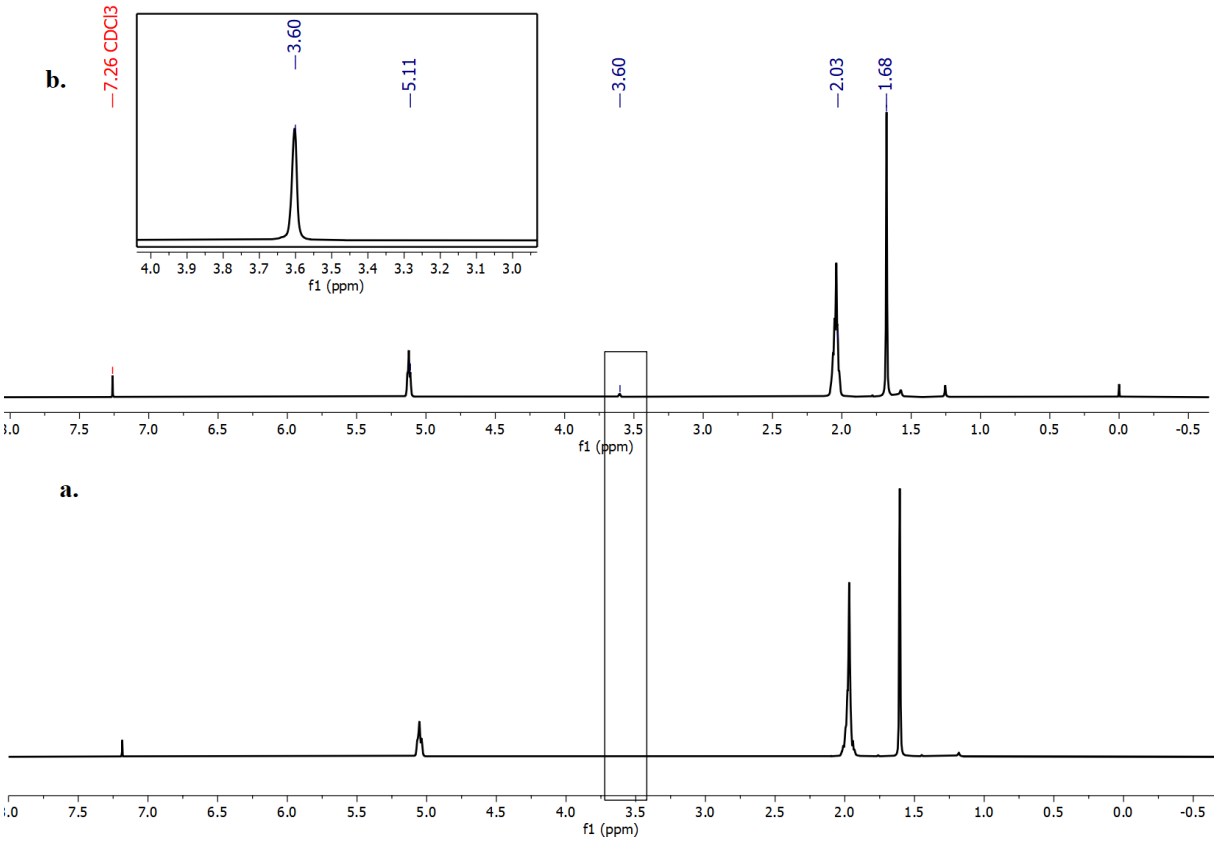

Fig. 2. ^{1}H NMR spectrum of (a) DPNR and (b) DPNR-g-PMMA

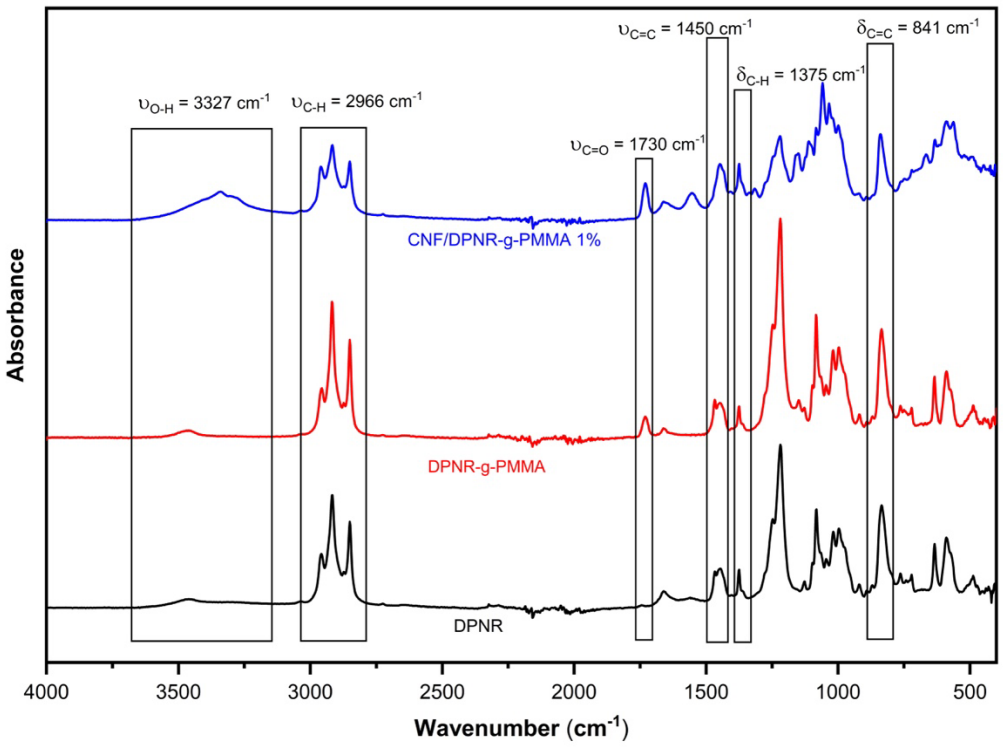

Fig. 3. FTIR spectra of DPNR, DPNR-g-PMMA and CNF/DPNR-g-PMMA 1%

In addition, the presence of cellulose in CNF/DPNR-g-PMMA material was proved by FTIR spectrum. Fig. 3 shows the FTIR spectrum of CNF/DPNR-g-PMMA with a very broad absorption band around 3345 cm^{-1}, which is typical for the vibration of hydroxyl groups. These groups indicated the presence of cellulose, which was incorporated into the natural rubber phase.

3.2. Thermal Properties of CNF/DPNR-g-PMMA Composite

The thermal properties of DPNR, DPNR-g-PMMA and their composites with varying CNF ratios were carried out using thermal gravimetric analysis and differential thermal gravimetric analysis (TGA-DTG) in a temperature range of 25 °C to 600 °C under a controlled nitrogen atmosphere. The findings of this study are displayed in Fig. 4 and 5. Under these conditions, only thermal degradation takes place, preventing the synergistic impact of thermal-oxidative degradation in the presence of oxygen. It appears that the thermal degradation process of DPNR, DPNR-g-PMMA, and CNF/DPNR-g-PMMA with varying CNF ratios becomes visibly altered at 200 °C and complete at 460 °C (Fig. 4).

The degradation process of the samples can be divided into three primary steps. The initial step, occurring within the temperature range of 200 °C to 340 °C, exhibits weight loss for DPNR, DPNR-g-PMMA, and CNF/DPNR-g-PMMA. This weight loss can be attributed to the evaporation of volatile components and primarily moisture. In the temperature range of 340 °C to 410 °C, a step of rapid pyrolysis occurs. During this step, most organic materials decompose, leading to the maximum weight loss. The second degradation step can be considered as the most significant indication for the thermal stability of rubber composites. In the final step, at temperatures above 470 °C, the volatile products of degradation are removed.

The data showed that the decomposition temperature (T_d) was elevated in DPNR-g-PMMA composites compared to DPNR. This disparity can be attributed to the existence of grafted PMMA segments along the DPNR chain, resulting in a reduction of the reactive unsaturated backbone and thus less susceptibility to degradation. Consequently, it is evident that grafting MMA enhanced the thermal stability of DPNR. This observation is consistent with the thermal degradation of modified natural rubber with other vinyl monomers. DPNR-g-PMMA and CNF/DPNR-g-PMMA samples with varying CNF ratios exhibited analogous degradation profiles. Nevertheless, T_d of CNF/DPNR-g-PMMA with varying CNF ratios is all higher than T_d of DPNR-g-PMMA. This improvement may be related to the larger interphase with restricted chain mobility generated due to the large surface area of nanocellulose and the entanglement of cellulose network. The restricted chain mobility delays the breakup of polymer chains as well as the loss of by-products. Overall, the incorporation of CNF into rubber composites led to an improvement in the thermal properties of these composites.

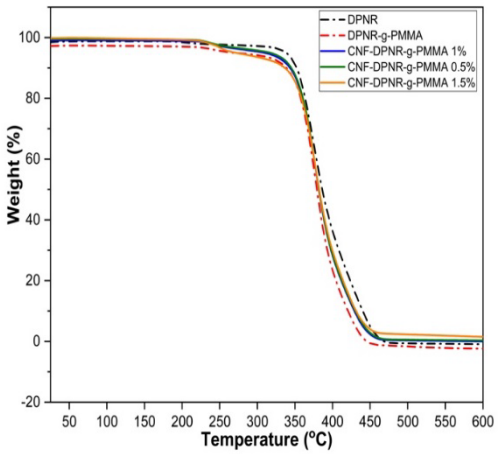

Fig. 4. TGA curves of DPNR, DPNR-g-PMMA and their composites with CNF in nitrogen

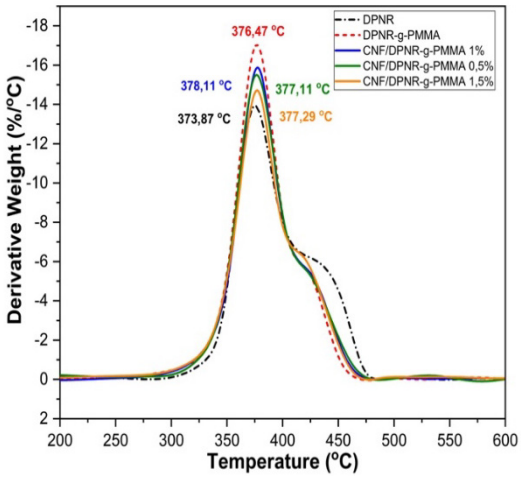

Fig. 5. DTG curves of DPNR, DPNR-g-PMMA and their composites with CNF in nitrogen

Additionally, it was noted that the concentration of CNF exerted an influence on the thermal stability of CNF/DPNR-g-PMMA composites. When incorporating CNF into DPNR-g-PMMA, the T_d for CNF/DPNR-g-PMMA at 0.5%, 1%, and 1.5% ratios were recorded as 377.11 °C, 378.11°C, and 377.29 °C, respectively. The T_d of CNF/DPNR-g-PMMA 1% is the highest and then shifts to lower temperatures with increasing nanocellulose content. Thomas *et al.* reported on the thermal degradation properties of CNF and natural rubber composites [16]. When using low ratios of the filler (0.5% - 1% CNF), a hydrogen bonding network was formed among the crosslinkers, CNF, and natural rubber. This network played a role in enhancing the thermal stability. However, at a higher filler percentage (1.5% CNF), there is a decrease in

thermal stability, which can be attributed to the fact that the degradation temperature of nanocellulose is relatively lower compared to that of the NR matrix. Moreover, the obvious surface polarity of the nanocellulose, which is due to the high content of hydroxyl groups, contributes to the agglomeration of the filler particles at higher weight percentages. The presence of oxygen in both the cellulose backbone and its side chains creates a conducive environment for the early thermal degradation of the rubber composite [17]. Therefore, the thermal stability can be improved to some extent at the lower filler percentage by reinforcing CNF in the natural rubber matrix.

After evaluating the thermal decomposition in nitrogen atmosphere, the thermal properties of the composites were further evaluated in the air atmosphere because NR is susceptible to thermal decomposition and oxidation when exposed to oxygen. Fig. 6 and 7 show the TGA and DTG curves of DPNR, DPNR-g-PMMA, and CNF/DPNR-g-PMMA with CNF ratios of 0.5%, 1%, and 1.5% in the air atmosphere.

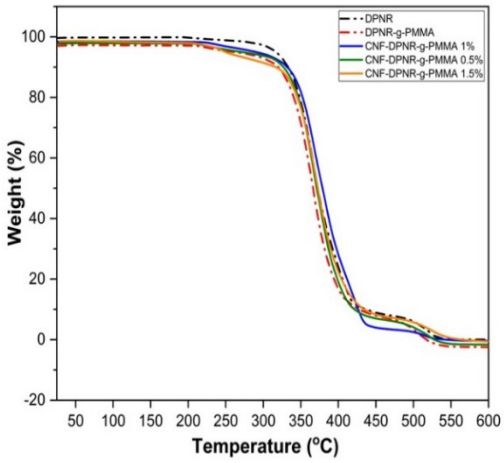

Fig. 6. TGA curves of DPNR, DPNR-g-PMMA and their composites with CNF in air

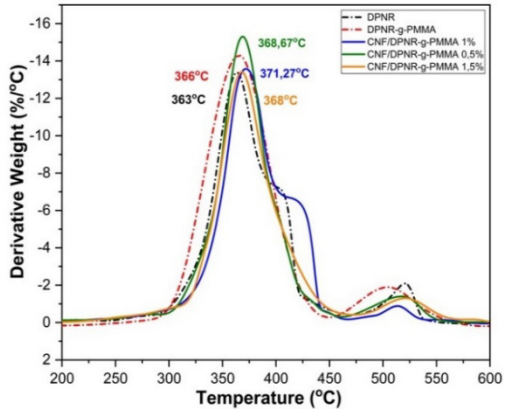

Fig. 7. DTG curves of DPNR, DPNR-g-PMMA and their composites with CNF in air

Under air atmosphere conditions, not only thermal decomposition occurs like in a nitrogen atmosphere, but also thermal oxidative decomposition occurs. Fig. 6 shows the thermal decomposition of DPNR, DPNR-g-PMMA, and CNF/DPNR-g-PMMA with varying CNF ratios occurring in the temperature range from 25 °C to 600 °C. The thermal decomposition process under air atmosphere conditions takes place similarly to that under nitrogen atmosphere conditions in the first two steps and is also divided into three main steps. The first step takes place in the temperature range from 200 °C to 330 °C, which shows a loss of mass due to the evaporation of volatile components and mainly moisture. The second step is the rapid pyrolysis stage, which takes place in the temperature range from 330 °C to 450 °C. In addition, in the final step, the thermal oxidative decomposition of the samples took place in the temperature range from 450 °C to 550 °C and during this process showed the formation of carbonaceous char.

Fig. 7 shows that the thermal decomposition of DPNR and DPNR-g-PMMA were presented at 363 °C and 366 °C, respectively, during the thermal decomposition step at about 300 °C-400 °C. The TGA and DTG curves of DPNR-g-PMMA and CNF/DPNR-g-PMMA with different CNF ratios in air atmosphere showed similar decomposition profiles. After the reinforcement of CNF to DPNR-g-PMMA, the decomposition temperature of CNF/DPNR-g-PMMA with ratios of 0.5%, 1%, and 1.5% is all higher than the decomposition temperature of DPNR-g-PMMA in the temperature range from 2.67 °C to 5.27 °C. Specifically, the T_d of CNF/DPNR-g-PMMA 0.5% is 368.67 °C, an increase of 2.67 °C compared to DPNR-g-PMMA. When the concentration of CNF was increased to 1.5%, the T_d of CNF/DPNR-g-PMMA 1.5% was 368 °C, which was almost unchanged compared with the T_d of CNF/DPNR-g-PMMA 0.5%. However, CNF/DPNR-g-PMMA 1% showed the highest thermal decomposition results among the three CNF ratios with a T_d of 371.27 °C. Besides, in the second thermal decomposition step at about 450 °C - 550 °C, the oxidation of NR and subsequent degradation of carbonaceous substances occurs. The amount of residue increased in the aerobic environment indicates the formation of carbonaceous char.

The TGA and DTG curves showed that in both air and nitrogen environments, the T_d of DPNR-g-PMMA is improved compared with DPNR. The improvement in thermal stability of rubber can be attributed to higher level of saturation obtained after the radical graft copolymerization [3]. Besides, it was found that when CNF was reinforced to DPNR-g-PMMA, the thermal stability of CNF/DPNR-g-PMMA was better than that of DPNR and DPNR-g-PMMA in both nitrogen and air atmosphere. From the analyzed results, in the nitrogen atmosphere, T_d of CNF/DPNR-g-PMMA is about 2 °C higher than the T_d of DPNR-g-PMMA

while in the air atmosphere, the T_d of CNF/DPNR-g-PMMA is about 5 °C higher than that of DPNR-g-PMMA. However, the results clearly show that the increase in thermal stability when increasing the CNF ratios from 0.5% to 1.5% was not very significant. It is expected that cellulose nanofibers are encapsulated by NR matrix and thereby have a delayed onset of decomposition. The increase of thermal stability for NR by the addition of CNF may be associated with the high amount of interphase with restricted chain mobility generated due to the large surface area of nanocellulose and the entanglement of CNF network [18]. Similar observations in previous studies also showed that the restricted chain mobility will retard the polymer chain scission as well as the loss of byproducts [19].

The glass transition temperatures (T_g) of the obtained materials were investigated with differential scanning calorimetry (DSC). The curves for DPNR, DPNR-g-PMMA, CNF/DPNR-g-PMMA 0.5%, CNF/DPNR-g-PMMA 1%, CNF/DPNR-g-PMMA 1.5% are presented in Fig. 7.

T_g is an important parameter in thermal analysis. It is mainly influenced by chain mobility, intermolecular reaction, branching and crosslinking degree. Fig. 8 illustrates how MMA and cellulose nanofibers (CNF) impact the glass transition temperature (T_g) of the rubber composites, as determined by DSC analysis. Evidently, the grafting of MMA led to a minor elevation in the glass transition temperature of DPNR (shifting from -62.64 °C for DPNR to -61.76 °C for DPNR-g-PMMA). The trend of the glass transition moving towards a slightly higher temperature indicates a limitation in the polymer chain mobility. The outcome was anticipated due to the presence of rigid PMMA branches resulting from polar interactions among ester groups. These branches limit the mobility of the isoprene main chain, causing a shift in T_g towards higher temperatures [3].

At various CNF ratios, the T_g of DPNR-g-PMMA is lower than the T_g of CNF/DPNR-g-PMMA. Specifically, the T_g of CNF/DPNR-g-PMMA with a 1% CNF ratio showed the the highest value at -59.54 °C and lower value of 0.5% and 1.5% ratios at -61.71 °C and -60.78 °C, respectively. These findings demonstrate that, in comparison to DPNR-g-PMMA, CNF/DPNR-g-PMMA's thermal characteristics are improved by reinforcement with CNF at various ratios. This may happen because the ester functional group ($COOCH_3$) on the side chain of the PMMA polymer matrix can interact with the hydroxyl groups of the cellulose nanoparticles. This contact may therefore prevent the polymer chains from rotating. Furthermore, the incorporation of small amounts of cellulose (0.5%, 1%, and 1.5%) into the rubber matrix leads to limitations resulting from the intermolecular bonding between the filler and the matrix. This constraint reduces the flexibility and mobility of polymer chains, leading to an increase in T_g. Besides, strong hydrogen bonding between the filler and the polymer matrices also lead to an improvement in T_g [20].

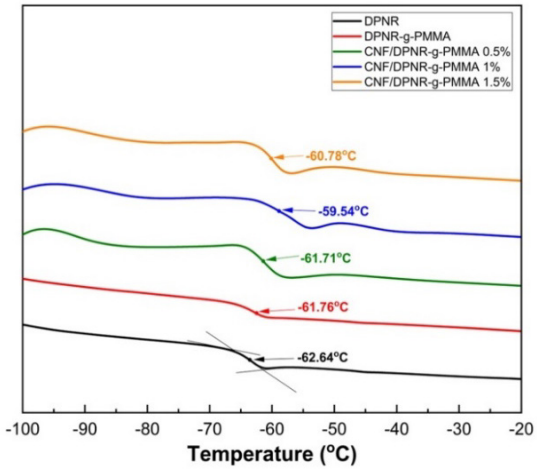

Fig. 8. DSC curves of DPNR, DPNR-g-PMMA, CNF/DPNR-g-PMMA 0.5%, CNF/DPNR-g-PMMA 1%, CNF/DPNR-g-PMMA 1.5%

4. Conclusion

In this study, the graft copolymerization of MMA onto DPNR and the process of dispersing CNF in DPNR-g-PMMA by ultrasonic waves to create composite materials have been successfully performed. The structures of DPNR-g-PMMA and CNF/DPNR-g-PMMA composites were characterized and confirmed by ^{1}H NMR and ATR-IR. The thermal decomposition of composites has been studied in both nitrogen and air atmospheres. Thermal decomposition in the nitrogen atmosphere consisted of a major step that showed better thermal stability of CNF/DPNR-g-PMMA compared with DPNR and DPNR-g-PMMA. The main two-step atmospheric thermal oxidative degradation also showed better thermal stability of the CNF-reinforced material compared with DPNR and DPNR-g-PMMA. These results prove that the incorporation of CNF into the DPNR-g-PMMA matrix increased thermal degradation and thermo-oxidative stability to some extent, especially this improvement depends on the concentration of CNF. Specifically, after reinforcing CNF to DPNR-g-PMMA, the decomposition temperature of the sample CNF/DPNR-g-PMMA 1% increased from 376.47 °C to 378.11 °C in nitrogen atmosphere and increased from 366 °C to 371.27 ° C in air atmosphere. Thus, CNF has a role in helping to improve the thermal stability of CNF/DPNR-g-PMMA materials compared to DPNR and DPNR-g-PMMA. In conclusion, composite materials from CNF and DPNR-g-PMMA have a potential to become promising materials in future research.

Acknowledgments

This research is funded by Asahi Glass Foundation, project No. AGF.2023-01.

Nguyen Thi Quynh acknowledges the kind support by the RoHan Project funded by the German Academic Exchange Service (DAAD, No. 57315854) and the Federal Ministry for Economic Cooperation and Development (BMZ) inside the framework "SDG Bilateral Graduate School programme".

References

[1] T. A. Dung *et al.*, Modification of Vietnam natural rubber via graft copolymerization with styrene, J. Braz. Chem. Soc., vol. 28, pp. 669-675, Apr. 2017. http://doi.org/10.21577/0103-5053.20160217.

[2] H. Nguyen Duy *et al.*, Improvement of thermal properties of Vietnam deproteinized natural rubber via graft copolymerization with styrene/acrylonitrile and diimide transfer hydrogenation, Polym. Adv. Technol., vol. 32, no. 2, pp. 736-747, Oct. 2021. https://doi.org/10.1002/pat.5126.

[3] T. N. Nguyen *et al.*, Improvement of thermal and mechanical properties of Vietnam deproteinized natural rubber via graft copolymerization with methyl methacrylate, Int. J. Polym. Sci., vol. 2020, pp.1-11, Jul. 2020. http://doi.org/10.1155/2020/9037827.

[4] B. Venugopal and J. Gopalakrishnan, Reinforcement of natural rubber using cellulose nanofibres isolated from Coconut spathe, Mater. Today: Proc., vol. 5, no. 8, pp. 16724-16731, Jan. 2018. http://doi.org/10.1016/j.matpr.2018.06.036.

[5] B. M. Cherian *et al.*, Cellulose nanocomposites with nanofibres isolated from pineapple leaf fibers for medical applications, Carbohydr. Polym., vol. 86, no. 4, pp. 1790-1798, Jul. 2011. https://doi.org/10.1016/j.carbpol.2011.07.009.

[6] T. Kunori and P. Geil, Morphology-property relationships in polycarbonate-based blends. I. Modulus, J. Macromol. Sci. Phys., vol. 18, no. 1, pp. 93-134, Jan. 1980. https://doi.org/10.1080/00222348008241375.

[7] K. Suthapakti *et al.*, Biodegradable compatibilized poly (l-lactide)/thermoplastic polyurethane blends: Design, preparation and property testing, J. Polym. Environ., vol. 26, pp. 1818-1830, May. 2018. https://doi.org/10.1007/s10924-017-1082-6.

[8] K. George *et al.*, Dynamic mechanical analysis of binary and ternary polymer blends based on nylon copolymer/EPDM rubber and EPM grafted maleic anhydride compatibilizer, Express Polym. Lett., vol. 1, Oct. 2007. http://doi.org/10.3144/expresspolymlett.2007.88.

[9] F. Okieimen and I. Urhoghide, Studies on miscibility of poly (vinyl chloride) with natural rubber-graft-polyacrylonitrile and natural rubber-graft-poly (methyl methacrylate), J. Appl. Polym. Sci., vol. 59, no. 11, pp. 1803-1808, Mar. 1996. https://doi.org/10.1002/(SICI)1097-4628.

[10] H. Afifi and A. El-Wakil, Study of the effect of natural rubber-graft-maleic anhydride (NR-g-MA) on the compatibility of NR-NBR blends using the ultrasonic technique, Polym. Plast. Technol. Eng., vol. 47, no. 10, pp. 1032-1039, Sep. 2008. https://doi.org/10.1080/03602550802355271.

[11] T. D. Cuong *et al.*, Study on antibacterial papermaking for food packaging using rice straw nanocellulose and nanochitosan, IOP Conf. Ser. Earth Environ. Sci., vol. 947, no. 1, pp. 012023, Dec. 2021. http://doi.org/10.1088/1755-1315/947/1/012023.

[12] E. Abraham *et al.*, Physicomechanical properties of nanocomposites based on cellulose nanofibre and natural rubber latex, Cellulose, vol. 20, pp. 417-427, Feb. 2013. https://doi.org/10.1007/s10570-012-9830-1.

[13] E. Abraham et al., X-ray diffraction and biodegradation analysis of green composites of natural rubber/nanocellulose, Polym. Degrad. Stab., vol. 97, no. 11, pp. 2378-2387, Nov. 2012. https://doi.org/10.1016/j.polymdegradstab.2012.07.028.

[14] O. Moussa, A. P. Vassilopoulos, and T. Keller, Experimental DSC-based method to determine glass transition temperature during curing of structural adhesives, Constr. Build Mater., vol. 28, no. 1, pp. 263-268, Mar. 2012. https://doi.org/10.1016/j.conbuildmat.2011.08.059.

[15] T. Nghiem Thi *et al.*, Preparation and properties of colloidal silica-filled natural rubber grafted with poly (methyl methacrylate), Polym. Bull., vol. 79, no. 8, pp. 6011-6027, Jun. 2022. https://doi.org/10.1007/s00289-021-03786-8.

[16] M. G. Thomas *et al.*, Nanocelluloses from jute fibers and their nanocomposites with natural rubber: Preparation and characterization, Int. J. Biol. Macromol., vol. 81, pp. 768-777, Aug. 2015. https://doi.org/10.1016/j.ijbiomac.2015.08.053.

[17] P. Gan *et al.*, Thermal properties of nanocellulose-reinforced composites: A review, J. Appl. Polym. Sci., vol. 137, no. 11, pp. 48544, Mar. 2020. https://doi.org/10.1002/app.48544.

[18] E. Abraham *et al.*, Green nanocomposites of natural rubber/nanocellulose: membrane transport, rheological and thermal degradation characterisations, Ind. Crops Prod., vol. 51, pp. 415-424, Nov. 2013. https://doi.org/10.1016/j.indcrop.2013.09.022.

[19] P. Visakh *et al.*, Crosslinked natural rubber nanocomposites reinforced with cellulose whiskers isolated from bamboo waste: Processing and mechanical/thermal properties, Compos. Part A Appl. Sci. Manuf., vol. 43, no. 4, pp. 735-741, Apr. 2012. https://doi.org/10.1016/j.compositesa.2011.12.015.

[20] M. Li *et al.*, Preparation and characterization of nanocomposite films containing starch and cellulose nanofibers, Ind. Crops Prod., vol. 123, pp. 654-660, Nov. 2018. http://doi.org/10.1016/j.indcrop.2018.07.043.